

Computational Fluid Analysis for High Lift on Multi-Element Airfoil Used in Civilian Aircraft

G.Parthasarathy¹, B. Shishira Nayana², B. Dinesh Kumar³

Associate Professor Aerospace engineering, PG. Scholar, PG.Scholar, MLR Institute of Technology, Hyderabad, India.

Abstract: The choice of high-lift system is crucial in the preliminary design process of a subsonic civil transport aircraft. Even a small increase in high-lift system performance can make a big difference in the profitability of the aircraft. A better understanding of high lift flows is needed to continue increasing the performance of high-lift systems while decreasing their complexity. The present work involves the design and aerodynamic analysis USING ANSYS CFX 14.5 of an multi-element airfoil with leading edge slat and trailing edge flap mostly used in transport aircrafts. Airfoil designed in 2D and 3D and analyzed in 3D for lift and drag coefficients at three different flap angles enhancing for the high lift.

Keywords: High lift devices, Flap,Slat, Aerodynamics, Ansys 14.5.

1. Introduction

The wing of an aircraft is classically designed to reach a desired performance at cruise conditions, which is transonic for current commercial aircraft. At landing or take-off, the aerodynamic conditions are so different that such wing cannot fulfill basic requirements without high-lift devices. The aim of such a system is to increase the lift coefficient in order to compensate the low velocity during the takeoff and approach phases.

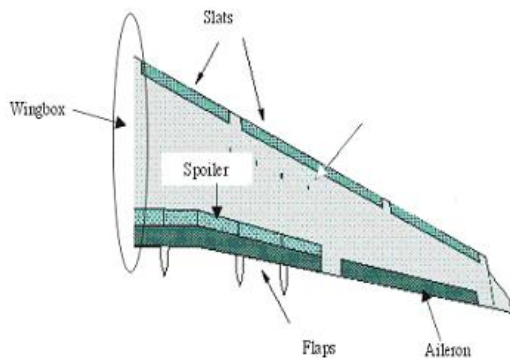


Figure 1: Wing with high lift devices flap and slat

The demands on the high-lift systems of future civil aircraft are numerous and challenging, for example reduced noise emissions, increased safety, reduced weight and reduced manufacturing and maintenance costs. Reduced noise emissions in itself is a serious challenge, including efforts to reduce both the airframe noise of high-lift configurations and to use different approach and landing procedures. To the deployment of trailing and/or leading edge devices the resulting multi-element wing can reach the necessary aerodynamic performance typically higher lift requested for a safe landing and take-off.

1.1 High-lift Configuration Airfoil

High-lift configuration normally constitute by leading edge device, main wing box and trailing edge device. The first and the third part calls High-lift devices, for their initial purpose used by engineering are to improve lift. Leading

edge device mainly increase the maximum lift on the wing by preventing wing leading edge stall increasing the maximum angle of attack, but it reduce the whole configuration lift when the AOA below medium. Currently, almost all the new civil airplane uses a full span of leading edge devices. Main wing box is the biggest part in the High-lift configuration; it does not just take the role as moments and forces taker, but also the main lift generator. Trailing edge devices decrease the zero lift AOA, for it increase the whole high-lift configuration airfoil camber, thus increase the lift for a given angle of attack as shows in Figure.

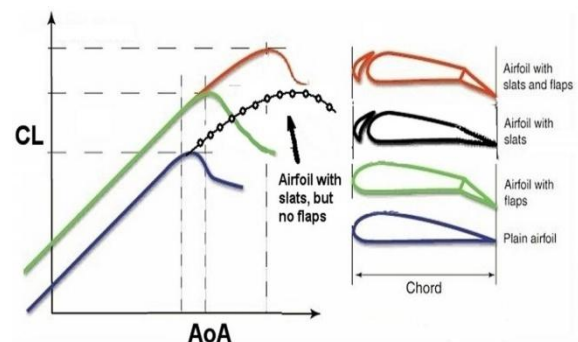


Figure 2 : The effect to lift coefficient from slat and flap

1.2 According to the boundary layer theory proved by Prandtl, when a Streamline object moves in a fluid, on the contact surface between object and fluid, there exists a thin to thick boundary layer from the front edge to the backward, at some distance, the airstream near the surface will reverse direction, form a separation between the main flow and the object's surface, according to Bernoulli's principle, so in order to conquer the viscosity effect that cause the separation, there exist just two ways to: increase the Pressure at the beginning of the upper surface, and the second is weaken or eliminate the viscosity boundary layer. That is the role that the High-lift devices play. Compared to a single airfoil, the High-lift airfoil should have at least one more portion. Generally, it has three or more portions to make the combination to be a high-lift airfoil.

An increase in camber

It is well known that cambered airfoil sections have a higher maximum lift coefficient than symmetrical sections. But airfoil camber also produces (at excessive camber excessive) drag. This is why, already in an early stage of aviation history, variable camber was employed in the form of split or plain flaps.

An increase in effective chord.

Deflection of a high-lift device can increase the effective chord length if there is a chord extension. A fixed-hinge flap with the hinge close to the chord line for example does not change the chord length, but a Fowler flap moves aft and does increase the effective chord. The same holds for a slat that usually moves down and forwards thereby increasing the effective chord length. Chord extension increases.

The mutual interaction effect

The lift on an airfoil section can be analyzed by replacing the actual section by a series of vortices on the section camber line. This series of vortices may vary between a continuous vortex sheet which allows the analysis of the chordwise lift distribution and a single vortex at the quarter chord position producing the total lift when the angle-of-attack is increased relative to the angle-of-attack for zero-lift, the zero-lift line. By means of Joukowski conformal transformations exact solutions without linearization can be obtained for the lift on a flat plate or a circle segment at any angle-of-attack.

Table 1: Values of CL_{max} for some airplanes

MODEL	CL_{max}
B-47/B-52	1.8
367-80/KC-135	1.78
707-320/E-3A	2.2
727	2.79
DC-9	3.0
747/E-4A	3.2
767	2.42
777	2.45

Clearly the 727 emphasized short fields, and thus required a higher CL_{max} . Anyone who ever looked out the window while landing in a 727 noticed the elaborate high lift system employed.

2. Methodology

2.1 CFD analysis on high-lift design

The aerodynamics around a wing in highlift configuration is one of the most complex flows occurring around an airplane. Fig. presents an example of the flow field around a wing section of a 3-element wing equipped with a slat at the leading edge and a flap at the trailing edge. Apart the typical boundary layer regions near the walls the multi-element wing presents additional important features like the recirculation areas in the cut-outs, the mixing of boundary layers and wakes of preceding elements and secondary flows that takes place through the slots between the main wing and high-lift devices. Furthermore, since the highlift wing operates at high-angle of attack, local supersonic area at the leading edge of the slat and flow separation is most likely to

occur on wing and flap upper sides. As a consequence the flow in high lift configuration is dominated by viscous effects. The most appropriate numerical method to correctly capture all these flow features in an acceptable turn around time must be based on compressible Reynolds-averaged Navier-Stokes (RANS) equations.

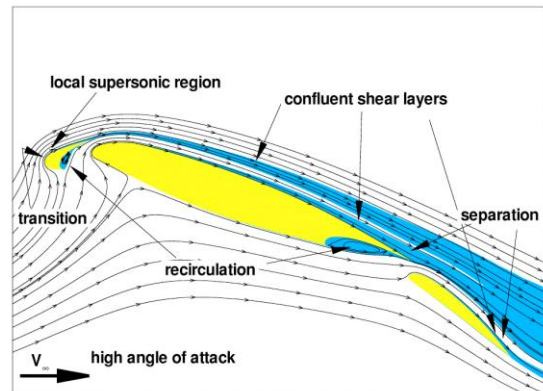


Figure 3: Flow field around the wing section of a 3-element wing

In order to capture all of these critical flow features a grid of high quality is required. This implies the use of thin cells not only normal to the wall for the accurate discretisation of the boundary layers but also behind the trailing edge of the upstream element and up to the downstream element in order to accurately resolve the wakes until its confluence with the boundary layer of the following elements. A thick layer of thin cells has then to be generated orthogonal to the wall in order to capture the mixing shear layers and the ability of the boundary layer to sustain separation. Furthermore, the high-lift configuration has complicated areas like slots, slat and flap coves, which have to be meshed as well. The selection of the meshing procedure for high-lift design is then a compromise between the flexibility to handle complex configurations, the number of cells for fast computations and the capability to control the space discretisation.

3. Geometry Model

To create 2D geometry in ANSYS Design Modeler, airfoil coordinates at root section are obtained by multiplying non-dimensionalized SC20610 data coordinates by root chord length. To cut flap and slat portions of airfoil, intermediate curve are created using splines in ANSYS and points are extracted from these curves.

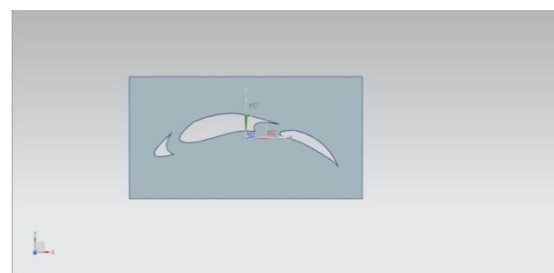


Figure 4: Geometry model with flap and slat open

3.1 Meshing

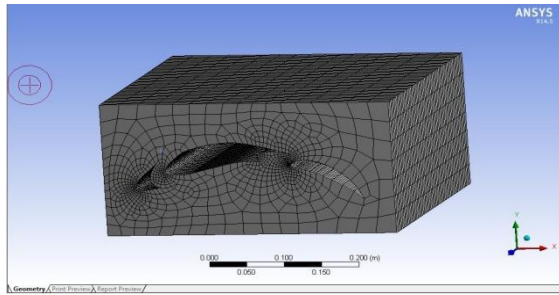


Figure 5: Meshed model: tet mesh,nodes-56463, elements 50344.

4. Fluent Analysis

Here the wing configuration with airfoil SC20610 is considered which is mostly used in the civilian aircraft with high payload and passenger capacity like BOEING and AIRBUS and are as follows.

Wing configuration:

Root Chord Length (c): 17.67 m, Taper Ratio: 0.26, Mid1 Chord Length @z = 7.929 m: 13.28 m, Wing Sweep: 33.5o, Mid2 Chord Length @z = 22.3814 m: 8.12 m, Slat Chord Length: 16% c, Tip Chord Length = 3.98 m, Flap Chord Length: 30% c. Wing Area = 845.417 m², Aspect Ratio: 7.5.

To perform CFD analysis, following specifications are given in Fluent 14.5

1. Velocity of A380: Takeoff = 280 km/h, Cruising = 900 km/h, Landing = 275 km/h.
2. Turbulence Model: Standard k-ε (2-eqn) is used as suggested in Reference [34].
3. Air Properties Used: Sea Level (SL) properties for takeoff & landing, High Altitude of 11430 m (HA)
4. Properties for cruising.
 Temperature = 15oC (SL) , -56.35 oC (HA)
 Density = 1.225 (SL), 0.34 kg/m³(HA)
 Pressure = 101,325 (SL), -80, 148 Pa (HA)
 Dynamic Viscosity = 1.783x10⁻⁵(SL), 1.42x10⁻⁵ kg/ms(HA)
5. Angle of Attack (α): To specify angle of attack, use $V_x = V \cos \alpha$ and $V_y = V \sin \alpha$.
6. Boundary Conditions are: (1) Velocity Inlet at V_x, V_y at left edge (2) Pressure Outlet at Atmospheric
7. Pressure at right edge (3) Free Surfaces at top and bottom edges.

Flap, Slat translations and rotations are obtained by applying transformation equations to slat and flap points.

(i) Flap Transformation equations with translation by (xoff, yoff) and rotation by θ .

$$x = c [(x - x_1) \cos \theta + y \sin \theta - (x_1 - x_{off})] \dots \dots (1)$$

$$y = c [-(x - x_1) \sin \theta + y \cos \theta] \text{ if } y_{off} = 0 \dots \dots (2)$$

(ii) Slat Transformation equations with translation by (xoff, yoff) and rotation by θ .

$$x = c [(x \cos \theta - y \sin \theta) + x_{off}] \dots \dots (3)$$

$$y = c [(x \sin \theta + y \cos \theta) + y_{off}] \dots \dots (4)$$

where for flap, xoff = 11.75% c, yoff = 0, θ (FA) = 16 deg; for slat, xoff = -7.57% c, yoff = -6.13% c, θ (SA) = +16 deg.

The velocity contour and pressure contour at three different flap angles are obtained by changing the the direction of the velocity stream as the boundary conhdion is free stream velocity.

4.1 Contours of pressure over SC20610N Airfoil

The static pressure of the air is simply the weight per unit area of the air above the level under consideration. For instance, the weight of the column of air with a cross-sectional area of 1 ft-square and extending upward pressure = 101.325 and for sea level 80 pa and high altitude pressure is increased to 148 pa .The amalgamation of static pressure and dynamic pressure is known as total pressure.

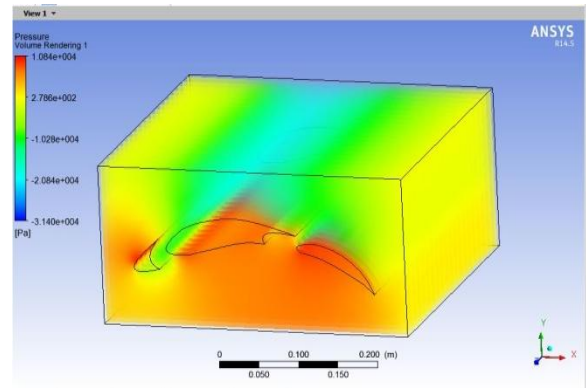


Figure 6: For zero degree flap angle the obtained pressure counter over an aerofoil slat, wing and flap.

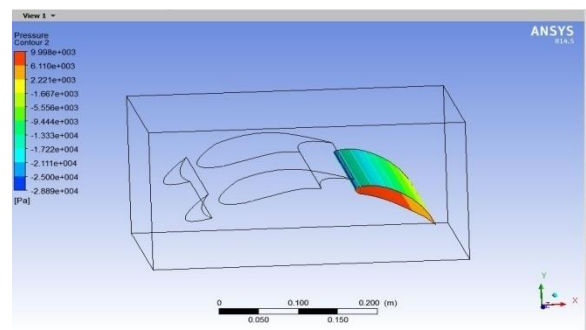


Figure 7: For the 16 degree flap angle the pressure counter over the airfoil

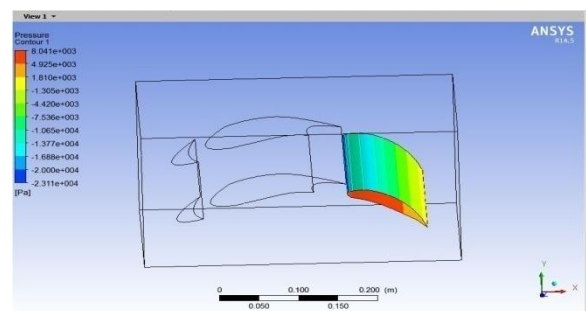


Figure 8: For the 30 degree flap angle pressure counter

4.2 Contours of Velocity magnitude over SC20610 airfoil

The velocity contours which create low velocity region at lower side of the airfoil and higher velocity acceleration region at the upper side of the airfoil and according to principle of Bernoulli's upper surface will gain low pressure

and lower surface will gain higher pressure. Hence value of coefficient of lift will increase and coefficient of drag will also increase but the increasing in drag is low compare to increasing in lift force.

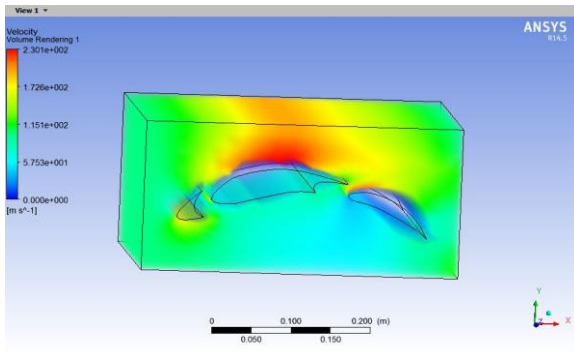


Figure 9: Velocity contour at zero flap angle

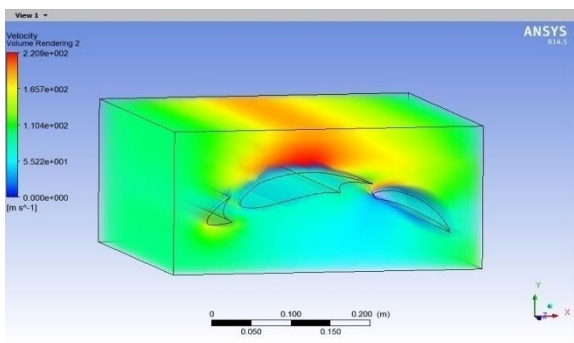


Figure 10: Velocity contour at 16 degree flap angle at 30 degree flap angle

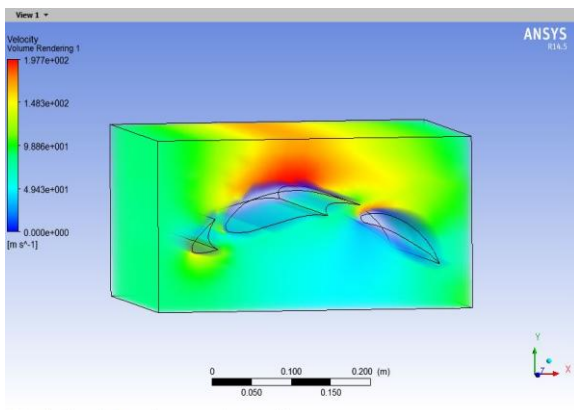


Figure 11: Velocity contour at 30 degree flap angle at 30 degree flap angle

5. Results

Table 2

AoA	FLAP ANGLE	LIFT COEFFICIENT	DRAG COEFFICIENT
8.53	0	108.7	2.51
8.53	16	340.7	17.99
8.53	30	405.3	37.2

6. Conclusion

When flap is lowered, it increases the effective angle of attack and generates increased lift. The effect of flap on the CL curve is to offset it in vertical direction. Lowering flap

reduces critical angle of attack. From the results obtained the lift coefficient is gradually increasing as the flap angle increases and same in the drag value. so it can be concluded that with flap angle change where the chord length changes resulting in the change in lift and drag. Flap angle with medium value can be used in takeoff condition and further more flap angle value conditions can be used in landing as the drag value is comparatively more.

References

- [1] Rudolph PKC., High-Lift Systems on Commercial Subsonic Airliners, NASA CR 4746, Sept. 1996.
- [2] Meredith PT., Viscous Phenomena Affecting High-Lift Systems and Suggestions for Future CFD Development, HighLift System Aerodynamics, AGARD CP-515, September 1993, pp.19-1--19-8.
- [3] Smith AMO., High-Lift Aerodynamics, AIAA Paper 74-939, Aug. 1974
- [4] Valarezo WO., Dominik CJ., McGhee RJ., Goodman WL., Paschal KB., Multi-Element Airfoil Optimization for Maximum Lift at High Reynolds Numbers, AIAA Paper 91-3332, Sept. 1991.
- [5] Valarezo WO., Dominik CJ., McGhee RJ., Reynolds and Mach Number Effects on Multi-element Airfoils, in Proceedings of the Fifth Numerical and Physical Aspects of Aerodynamic Flows, California State University, Long Beach, CA, Jan. 1992.
- [6] Chin VD., Peters DW., Spaid FW., McGhee RJ., Flowfield Measurements About A Multi-Element Airfoil At High Reynolds Numbers, AIAA Paper 93-3137, July 1993.
- [7] Storms BL., Ross JC., An Experimental Study of Lift-Enhancing Tabs on a Two-Element Airfoil, AIAA Paper 94-1868, June 1994.
- [8] Horton HP., Fundamental Aspects of Flow Separation Under High-Lift Conditions, von Karman Institute for Fluid Dynamics, Brussels, Belgium, 1970.
- [9] Nakayama A., Kreplin HP., Morgan HL., Experimental investigation of flowfield about a multi-element airfoil, AIAA Journal, V26, pp. 14-21, 1990.
- [10] van Dam CP., The aerodynamic design of multi-element high-lift systems for transport airplanes, Progress in Aerospace Sciences, Vol 38, pp 101-144, 2002.

Author Profile

B.Shishira Nayana pursuing Master's degree in Aerospace engineering from M.L.R college of Engineering and Technology (2013-2015). She received Bachelor's degree in Aeronautical Engineering from Malla Reddy Engineering and Technology, JNTU Hyderabad in 2012. Interested in Aerodynamic analysis and undergone the internship program in CFD with ALTAIR Acusolve in 2013.